Received: 20 December 2016 | Revised: 13 January 2017 | Accepted: 19 January 2017

DOI 10.1002/ajmg.a.38170

ORIGINAL ARTICLE

AMERICAN JOURNAL OF WILEY medical genetics PART A

# The phenotypic spectrum of congenital Zika syndrome

Miguel del Campo[1,*] | Ian M. L. Feitosa[2,3,*] | Erlane M. Ribeiro[4] | Dafne D. G. Horovitz[5] | André L. S. Pessoa[4] | Giovanny V. A. França[6] | Alfredo García-Alix[7] | Maria J. R. Doriqui[8] | Hector Y. C. Wanderley[9] | Maria V. T. Sanseverino[10] | João I. C. F. Neri[11] | João M. Pina-Neto[12] | Emerson S. Santos[13] | Islane Verçosa[14] | Mirlene C. S. P. Cernach[15] | Paula F. V. Medeiros[16] | Saile C. Kerbage[4] | André A. Silva[2,10,17] | Vanessa van der Linden[18] | Celina M. T. Martelli[19] | Marli T. Cordeiro[19] | Rafael Dhalia[19] | Fernanda S. L. Vianna[2,10] | Cesar G. Victora[20] | Denise P. Cavalcanti[21,†] | Lavinia Schuler-Faccini[2,11,†] | on behalf of Zika Embryopathy Task Force—Brazilian Society of Medical Genetics ZETF-SBGM

[1] Division of Dysmorphology and Teratology, Department of Pediatrics, UCSD, San Diego, California

[2] Departamento de Genetica, Universidade Federal de Rio Grande do Sul, Porto Alegre, Rio Grande do Sul, Brazil

[3] Departamento de Medicina Clínica, Universidade Federal de Pernambuco, Recife, Brazil

[4] Hospital Infantil Albert Sabin, Fortaleza, Ceara, Brazil

[5] Instituto Fernandes Figueira, Fundação Oswaldo Cruz, Rio de Janeiro, Brazil

[6] Secretariat of Health Surveillance, Ministry of Health, Brasilia, Brazil

[7] Institut de Recerca Pediàtrica Sant Joan de Déu, Universitat de Barcelona, Barcelona, Spain

[8] Hospital Infantil Dr. Juvêncio Mattos, São Luiz, Brazil

[9] Secretaria de Estado da Saúde do Espírito Santo, Vitória, Brazil

[10] SIAT—Brazilian Teratogen Information Service, Medical Genetics Service, Hospital de Clinicas de Porto Alegre, Porto Alegre, Rio Grande do Sul, Brazil

[11] Universidade Potiguar, Natal, Brazil

[12] Faculdade de Medicina de Ribeirao Preto, Departamento de Genetica, Universidade de Sao Paolo, Ribeirao Preto, Brazil

[13] Universidade Federal de Sergipe, Lagarto, Brazil

[14] Centro de Aperfeiçoamento Visual Ver a Esperança Renascer/CAVIVER, Fortaleza, Brazil

[15] Departamento de Genetica Medica, Universidade Federal de Sao Paolo (UNIFESP), Sao Paolo, Brazil

[16] Universidade Federal de Campina Grande, Campina Grande, Paraiba, Brazil

[17] UNIVATES University, Porto Alegre, Rio Grande do Sul, Brazil

[18] Associação de Assistência à Criança Deficiente/AACD, Recife, Brazil

[19] Centro de Pesquisas Aggeu Magalhães, Fundação Oswaldo Cruz, Recife, Brazil

[20] Graduate Program in Epidemiology, Federal University of Pelotas, Pelotas, Rio Grande do Sul, Brazil

[21] Departamento de Genetica Medica, Universidade de Campinas UNICAMP, Campinas, Brazil

*These authors have contributed equally to the study and manuscript.

†These authors contributed equally to the study and manuscript.

  

**Correspondence**
Miguel del Campo MD, PhD, UCSD, Department of Pediatrics, 9500 Gilman Dr, MC0828, La Jolla, CA 92093-0828.
Email: midelcampo@ucsd.edu
Lavinia Schuler-Faccini, Departamento de Genetica/Universidade Federal do Rio Grande do Sul, Serviço de Genética Médica/Hospital de Clinicas de Porto Alegre, Caixa Postal 15053—Ag, Campus Agronomia CEP 91501-970, Porto Alegre, Rio Grande do Sul, Brazil.
Email: lavinia.faccini@ufrgs.br

**Funding information**
Conselho Nacional de Desenvolvimento Científico e Tecnológico, Grant number: 306489/2010-4; Brazilian Society of Medical Genetics

In October 2015, Zika virus (ZIKV) outbreak the Brazilian Ministry of Health (MoH). In response, the Brazilian Society of Medical Genetics established a task force (SBGM-ZETF) to study the phenotype of infants born with microcephaly due to ZIKV congenital infection and delineate the phenotypic spectrum of this newly recognized teratogen. This study was based on the clinical evaluation and neuroimaging of 83 infants born during the period from July, 2015 to March, 2016 and registered by the SBGM-ZETF. All 83 infants had significant findings on neuroimaging consistent with ZIKV congenital infection and 12 had confirmed ZIKV IgM in CSF. A recognizable phenotype of microcephaly, anomalies of the shape of skull and redundancy of the scalp consistent with the Fetal Brain Disruption Sequence (FBDS) was present in 70% of infants, but was most often subtle. In addition, features consistent with fetal immobility, ranging from dimples (30.1%), distal hand/finger contractures (20.5%), and feet malpositions (15.7%), to generalized arthrogryposis (9.6%), were present in these infants. Some cases had milder microcephaly or even a normal head circumference (HC), and other less distinctive findings. The detailed observation of the dysmorphic and neurologic features in these infants provides insight into the mechanisms and timings of the brain disruption and the sequence of developmental anomalies that may occur after prenatal infection by the ZIKV.

**KEYWORDS**
congenital Zika infection, congenital Zika sequence, congenital Zika syndrome, disruption, disruptive sequence, dysmorphology, fetal brain disruption sequence, teratogen, teratology, Zika virus

## 1 | INTRODUCTION

Following its identification in the Zika forest in Uganda in 1947, the mosquito borne flavivirus Zika virus (ZIKV) migrated until arriving and quickly spreading in northeastern Brazil and other regions of the country in 2015 (Brasil, Calvet, et al., 2016; Campos, Bandeira, & Sardi, 2015; Dick, 1952). The ZIKV has now been recognized as being present in most countries in North America, the Caribbean, and Latin America, with strong evidence of vertical transmission during all three trimesters of pregnancy (Fauci & Morens, 2016). Astute clinicians in Northeast Brazil initially observed an increase in the number of cases of congenital microcephaly in their cities. This was followed by their hypothesis that prenatal infection by the ZIKV could be causative and led the Brazilian Ministry of Health (MoH) to recommend official ascertainment, surveillance, and expert evaluation of all notified cases (PAHO, 2015). In December 2015, the Brazilian Society of Medical Genetics (SBGM in Portuguese) established the SBGM Zika Embryopathy Task Force (SBGM-ZETF) in order to describe the phenotype of incident cases of prenatal ZIKV infection, understand the mechanisms leading to the observed features, and collect data on the natural history of the disorder. At the end of January 2016, the main clinical and phenotypic findings in 35 infants, including physical, neurologic, and neuroimaging features, were briefly reported, suggesting a specific phenotype for these infants that included but also extended beyond microcephaly (Schuler-Faccini, Ribeiro, et al., 2016). More recently, brain imaging findings have been described in detail and appear to include a characteristic neuroanatomic profile (Brasil, Pereira, Moreira, et al., 2016; de Fatima Vasco Aragao et al., 2016; Guillemette-Artur, Besnard, Eyrolle-Guignot, Jouannic, & Garel, 2016; Hazin et al., 2016; Soares de Oliveira-Szejnfeld et al., 2016). Ocular involvement has also been described in detail (de Paula Freitas et al., 2016; Miranda et al., 2016; Ventura, Maia, Bravo-Filho, Góis, & Belfort, 2016; Ventura, Maia, Travassos, et al., 2016; Ventura, Maia, Ventura, et al., 2016). Recent comprehensive reviews have synthesized the existing evidence regarding the multiple clinical components of Congenital Zika Syndrome (De Barros Miranda-Filho et al., 2016; Moore et al., 2016). These major components, also reflected in the findings outlined in this manuscript, include dysmorphic features and contractures, altered neurologic function, changes in brain structure, and ocular lesions.

This study reports data collected on 83 children with presumed or confirmed ZIKV congenital infection. We describe the observed phenotypic range in these infants, analyze and discuss in greater detail the dysmorphic and neurologic findings, and attempt to explain their pathogenesis. We identified a distinct yet variable phenotype that should be clinically recognizable in new cases of the infection, and guide confirmatory testing including brain imaging, viral, and serologic studies.

## 2 | METHODS

### 2.1 | Study oversight

A multi-center protocol for the investigation of the phenotype was approved by the Brazilian National Ethics Committee under the

registration CAEE 56176616210015327. All participants provided full written informed consent for data collection and registration. Most additionally consented to photographic and video documentation for review and publication.

## 2.2 | Study population

More than 200 patients with head circumference (HC) ≤33 cm were registered and examined by the SBGM-ZETF. Of these, only those 83 live-born infants with brain imaging (CT scan and/or MRI) consistent with ZIKV prenatal infection were included in the final analysis. The rest were excluded either because they had normal HC and normal postnatal exam and development, or because another cause of microcephaly was suspected or identified. Additionally, 49 cases were excluded because the available documentation, particularly brain imaging, was not considered sufficient. The HC cut-off criterion for enrollment (HC ≤33 cm) followed the December 2015 first version of the protocol of the MoH in Brazil for ascertainment. The registered infants were born between July 2015 and March 2016 in 10 different Brazilian states. The infants were examined between 0 and 10 months of age. Most (27/35) of the infants previously reported by Schuler-Faccini, Ribeiro, et al. (2016) were included in this study. In summary, and as detailed further below, the 83 infants included in the final analysis demonstrated cerebral calcifications, abnormal gyral patterns, and/or ventriculomegaly and increased extra-axial space, consistent with ZIKV congenital infection.

## 2.3 | Data collection, physical, and neurological examinations

All infants were examined by at least one clinical geneticist with experience in Dysmorphology, and, when available, their clinical photos, videos and brain imaging were reevaluated and discussed by others: at least 40 cases were examined by two or more clinical geneticists; three neonatal/pediatric neurologists also examined 68% of the infants. Clinical geneticists followed standardized protocols described below. Later in the study, changes were made to the exam protocol based on acquired experience.

Data collected included family history, prenatal information on maternal infection, exposures to other potential teratogens and diseases in pregnancy and TORCH serologies (toxoplasma, rubella, CMV, herpes simplex and syphilis). Z-scores were calculated for birth length (BL), birth weight (BW), and birth HC using InterGrowth reference charts (Villar et al., 2014). The physical examination consisted of a full evaluation of major and minor birth defects following the methods and norms of dysmorphology. All clinical geneticists also performed a standardized neurological exam. Three neonatal/pediatric neurologists also reviewed clinical videos of some of the other infants that they had not examined.

## 2.4 | Eye exams

Complete ophthalmologic examinations performed in these infants will be published elsewhere.

## 2.5 | Brain and skull imaging

Cranial CT and/or MRI were available on all infants. Brain images were photographed and reviewed. Reconstructed CT of the skull were available for three infants.

## 2.6 | Confirmation of congenital infection by the ZIKV

Zika virus IgM enzyme-linked immuno-sorbent assay (ELISA) in cerebrospinal fluid (CSF) were available in 14 of these infants based on the current recommendations for diagnosis of congenital ZIKV infection (Cordeiro, Pena, Brito, Gil, & Marques, 2016; Russell et al., 2016).

## 2.7 | Statistical analysis

Fisher's two-tailed exact test was used to compare dysmorphic, neurological, and cerebral findings in the three different groups of Z scores of HC. The Pearson correlation coefficient was calculated for correlation of measures of HC, BL, and BW. Statistical analysis was carried out using the Stata 13 software (StataCorp. 2013. Stata Statistical Software: Release 13. Collefe Station, TX: StataCorp LP).

# 3 | RESULTS

The detailed data collected for each of the 83 cases is shown in Supplemental Table S6.

## 3.1 | Family and pregnancy history

Fourth degree parental consanguinity (first cousins) was reported in only one case. No family history of microcephaly or developmental problems was elicited. A history of cutaneous rash (77%), associated with at least one additional symptom (73.5%) such as fever, conjunctival hyperemia, itching, or arthralgias lasting 2–4 days was recalled by the mothers of these infants. Fever had been low grade, and lasted 3–4 days. The recalled gestational ages of the presumed ZIKV infection ranged from 1 to 8 months of pregnancy, with a mean of 3.1 months. Father's previous infection was not queried, though in two pregnancies fathers reported having a rash, while the mothers did not experience any symptoms. No exposures to known human teratogens were disclosed and none of the mothers had significant health problems affecting the pregnancy. TORCH serologies, available in the majority of cases, ruled out other congenital infections included in the TORCH panel in all of those tested. The study group included more female (47/83, 57%) than male infants. Prematurity (gestational age less than 37 weeks) was observed in 18 (22.5%) of all study newborns. Of those 18 infants, one was born at 31 weeks, another at 32 weeks, the remainder between 34 and 37 weeks (Table 1).

**TABLE 1** Pregnancy data of the 83 infants

| | *N* | % |
|---|---|---|
| More than one recalled symptom among fever, rash, arthralgia, itch, conjunctival hyperemia | 61 | 73.5 |
| Maculopapular rash | 64 | 77.1 |
| TORCH negative confirmed | 59 | 71.1 |
| Prematurity (GA <37 weeks) | 18 | 22.5 |
| | Mean | Range |
| Maternal age (years) | 26.1 years | 16–41 years |
| Paternal age (years) | 29.5 years | 18–53 years |
| Recalled gestational age at the time of the rash (months) | 3.1 months | 1–8 months |

## 3.2 | Growth and HC

Measurements at birth were available for review for almost all infants. BW was missing in three infants, BL in six, birth HC in four. Although the majority of newborns had normal BL and BW, 41.8% had decreased length and 18.7% had weight values below −2 Z scores. The mean HC at term was 29.1 cm (−2.8 SD). HC was below −3 SD in 57.4% of the cases, but 24.6% of newborns did not have microcephaly (HC ≥−2SD). HC at the time of the exam identified microcephaly that was not present at birth in at least four infants included in the study. In many cases head size was difficult to measure due to the abnormal skull shape, particularly the occipital prominence. There were significant correlations between values of HC and BL (correlation coefficient 0.338, $P = 0.003$), and HC and BW (correlation coefficient 0.494, $P = 0.001$) (Table 2).

## 3.3 | Dysmorphic features

The frequencies of all dysmoprpic features are shown in Table 3.

### 3.3.1 | Face

A general appearance of craniofacial disproportion was identified in 76 infants (96%) in the study population. A small HC and a decrease in the vertical size of the skull were evident in most cases. The smaller skull resulted in a sloping forehead with prominence of the supraorbital ridges, creating the appearance of proptosis and oversized facial features. With the exception of a few outliers, the palpebral fissures, the inner- and outer-canthal distances, the length and configuration of the philtrum, the shape of the lips and the size and shape of the ears were all normal. The periorbital tissues appeared full in many cases, and the eyelashes long, although these observations were not quantified. Epicanthal folds with bulging redundancy of the skin over the nasal bridge extending downward from the glabella were seen in four patients. A depression in the glabella region due to folding of the redundant skin was sometimes present. Retrognathia was present in 38.6%, and was most often mild. Only a few cases of severe micrognathia were seen, particularly in conjunction with arthrogryposis. None of the children 6–10 months of age had erupted teeth. The alveolar processes were often broad posteriorly, creating an apparently narrow palatal vault and the sublingual frenulum was absent in 4/11 infants in which it was assessed (Figures 1 and 2; Tables 2 and 3).

### 3.3.2 | Skull shape

The fontanelles were very small or apparently closed at birth in 21 infants (25.3%), the sutures (coronal, temporal, lambdoid) were uneven or overlapping in 18 (21.7%), and the prominent metopic ridge gave an appearance of severe trigonocephaly in eight cases (9.6%). The bifrontal diameter was narrow with a central bulge and bilateral depressions were present in 56.6% of the patients. The parietal bones were also deficient often leading to a prominent sagittal suture. The superior half of the squamous portion of the temporal bones and the parietal bones were also depressed, creating what we termed a "supratemporal depression." One particularly evident feature was posterior bulging of the occipital bone; the occipital prominence extended in the most severe cases 4–6 cm in the horizontal plane and 2–3 cm along the vertical axis of the back of the skull, but less so in most cases. The occipital prominence could be easily seen in 30% of the cases and felt in many more. Although one or more of these skeletal features were present in the majority of cases (69.7%), they were difficult to quantify, and appeared to follow a continuum. In the more severe cases the cranial anomalies were easily observed, including by palpation. Uneven and overlapped sutures were also obvious on simple CT and the shape of the skull confirmed its external evaluation when reconstructed 3D cranial CT studies were available as shown in Figure 3.

### 3.3.3 | Redundancy of the skin of the scalp and body

There was loose and redundant skin in some area of the scalp in 67.4% of infants. The redundant skin was not thickened. In 38.6% of the infants, we were able to demonstrate redundant skin over the entire calvarium, with visible scalp rugae (cutis rugata), or occasionally with a

**TABLE 2** Mean and standard deviation of the head circumference (HC), length, and weight at birth (for the total sample/and for IgM+ cases only), the SD of the mean, and the distribution in three ranges of Z-scores, in all infants born at term (≥37 weeks)

| | | | | *N* (%) | | |
|---|---|---|---|---|---|---|
| | *N* | Mean total/IgM+ | SD | <−3 SD | ≥−3 SD to ≤−2 SD | >−2 SD |
| HC (cm) | 61 | 29.1/29.7 | 2.8 | 35 (57.4) | 11 (18.0) | 15 (24.6) |
| Length (cm) | 58 | 45.2/45.7 | 3.7 | 8 (13.8) | 16 (27.6) | 34 (58.6) |
| Weight (g) | 59 | 2695/2762 | 455.3 | 1 (1.7) | 10 (17.0) | 48 (81.3) |

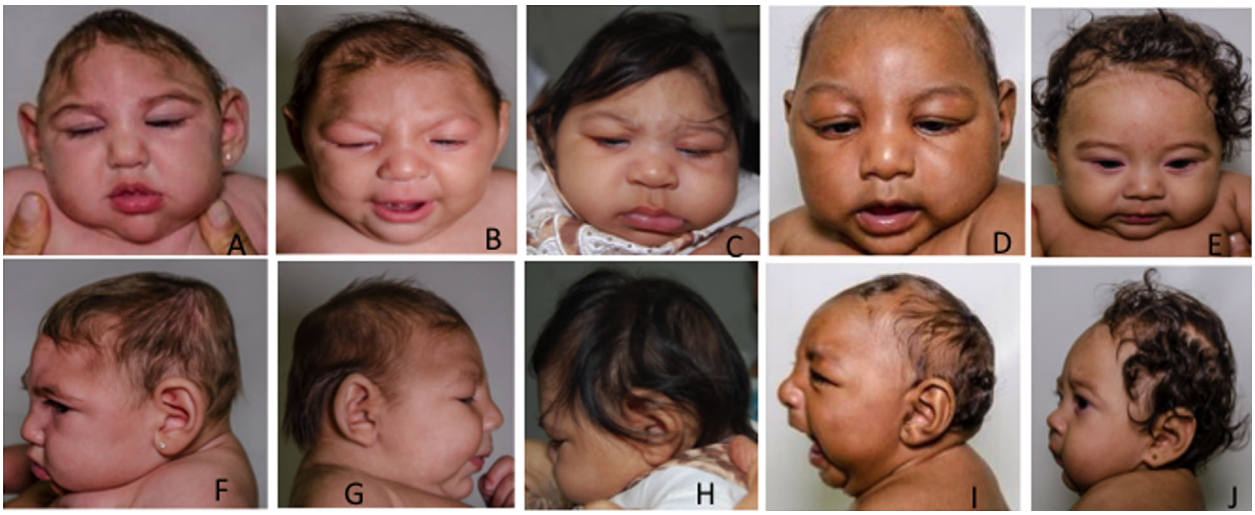


**FIGURE 1** Frontal and profile views of five children with congenital Zika syndrome showing varying degrees of craniofacial disproportion and abnormal skull morphology. Significant abnormalities of the cranium are seen in some infants, such as narrow and laterally depressed frontal bone (A–C) and occipital prominence (F and G). In other infants (D, E, I, J), less severe microcephaly and more subtle features were observed. In a third patient, a narrow bifrontal diameter is observed (C) but no occipital prominence is seen (H), and a fourth patient, has a normal frontal region (D) and a subtle occipital prominence (I). These observations indicate that cranial shapes vary greatly among patients. The eyes are closed in most children, and periorbital fullness, epicanthal folds, and mild retrognathia are the main facial features of these infants. [Color figure can be viewed at wileyonlinelibrary.com]

cerebriform shape (cutis gyrata). Redundant skin could be best demonstrated by manually creating folds in the scalp. Redundant skin was particularly evident in the forehead (37.3%) or in the occipital and nuchal regions (47%). In the glabellar region redundant skin created bulging vertical furrows, which was more obvious when the infant cried; these furrows extended downward, sometimes creating significant epicanthal folds. Horizontal folds over the occipital bony prominence extended downward to the nuchal region and upper back, creating the appearance of a short neck. The skin over the body and limbs appeared loose and created folds in five cases, a feature difficult to quantify (Figure 4).

Both the irregularities of the cranial shape mentioned above, and the redundancy of the skin were less severe in infants older than 3 months; a trend toward milder skull and scalp anomalies with time was noted by the examiners.

### 3.3.4 | Hair patterning and whorls

Hair patterns were observed as normal in 94%. However, in five cases (6%), abnormal scalp hair patterning such as frontal upsweeps, frontal hair whorls, double misplaced hair whorls, or excessively lateralized posterior hair whorls were identified (Figure 5).

### 3.3.5 | Joint contractures, dimples, and creases

Significant contractures of at least one joint were present in 35/83 (42.1%), although Arthrogryposis multiplex congenita was seen only in 10% or cases. Wrist and digital contractures (wrist malposition and camptodactyly, 20.5%) and foot malposition (equinovarus to talus valgus, 15.7%), often not reducible, or a prominent calcaneous (7.2%), were seen. Abnormal hand creases, such as single transverse palmar creases, were seen in five cases. Deep palmar creases were often

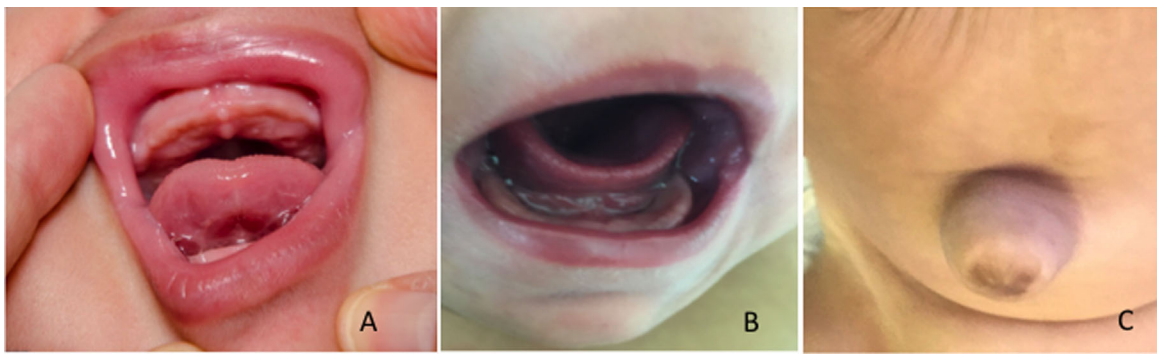


**FIGURE 2** Increased thickness of the posterior aspect of the alveolar ridge (A), absence of the sublingual frenulum (B) and small umbilical hernia (C). [Color figure can be viewed at wileyonlinelibrary.com]

**TABLE 3** Dysmorphic features in 83 infants with ZIKV prenatal infection

| Findings | *N* | % | IgM+ CSF (*N* = 12) |
|---|---|---|---|
| Facial dysmorphic features | | | |
| Craniofacial disproportion | 76 | 91.6 | 12 |
| Epicanthal folds | 4 | 4.8 | 1 |
| Retrognathia | 32 | 38.6 | 3 |
| Redundant skin | | | |
| Excess skin over the entire scalp | 32 | 38.6 | 4 |
| Excess skin only over the forehead | 31 | 37.3 | 5 |
| Occipital and nuchal skin folds | 39 | 47 | 6 |
| Short appearing neck | 28 | 33.7 | 0 |
| Abnormal skull shape | | | |
| Narrow forehead with bilateral depressions | 47 | 56.6 | 4 |
| Prominent metopic or sagittal suture | 8 | 9.6 | 1 |
| Supratemporal depression | 25 | 30.1 | 2 |
| Large visible occipital prominence | 25 | 30.1 | 4 |
| Closed fontanelles | 21 | 25.3 | 6 |
| Overlapped sutures | 18 | 21.7 | 7 |
| Hair | | | |
| Abnormal hair patterns and whorls | 5 | 6 | 3 |
| Contractures | | | |
| Hand contractures/ camptodactyly | 17 | 20.5 | 4 |
| Feet contractures | 13 | 15.7 | 2 |
| Prominent calcaneous | 6 | 7.2 | 1 |
| Multiple dimples | 25 | 30.1 | 5 |
| Multiple arthrogryposis | 8 | 9.6 | 2 |

observed. Hands with finger camptodactyly demonstrated sometimes faint interphalangeal creases. Excessive dimpling (two dimples per joint or larger flexion creases) were seen in 30.1% of the infants, often over multiple joints, particularly over the wrists, elbows, knees, and ankles, less frequently over the shoulders and hips (Figure 6).

## 3.4 | Neurologic findings

Three main features were seen in most infants and were more evident in those younger than 3 months of age: alterations of motor activity (tone, posture, and motility), abnormal neurobehaviour, and excitability (Table 4 and Figure 7).

Generalized hypertonia was present in 74.7% of patients, leading to axial extensor postures, or flexor postures, in 27.7% of the infants. There were abnormal positions (flexed, hyperextended, or laterally deviated) of the wrists. Even in the absence of fixed contractures, the fists were clenched and the fingers were difficult to extend. Excessive thumb adduction was often present. Flexion of other fingers was observed, particularly at the index, with flexion of the distal two phalanges over the proximal phalanx. A reduction of spontaneous movements—motor hypoactivity—and alterations of their quality were consistent findings in almost all infants, although this feature was not systematically quantified.

There was poor and delayed overall response to contact with the examiner. Although visual tracking was usually present, it was inconsistent and of short durations. In some infants the eyes were often closed during the entire exam. Responses to auditory stimuli were present but occasionally appeared decreased or inconsistent. Audiologic testing (otoacoustic emission and brainstem evoked responses BER or ABR test) have confirmed abnormal hearing in a few infants (results not shown).

Soon after beginning the physical exam, the babies demonstrated irritability with excessive crying, and were often inconsolable. The pattern of the cry was sometimes poorly modulated, and was often divided into short bursts that appeared monotonous. Umbilical hernias were present in many children with irritability and inconsolable crying. Some mothers reported persistent crying for weeks with poor response to any soothing maneuvers. Coarse stimulus-sensitive tremor, excessive startles, and hyperactive myotatic reflexes and clonus were often elicited by the exam.

In infants older than 3 months, there was persistence of primitive neonatal responses (Moro, sucking, rooting, and tonic asymmetric response). Almost no spontaneous fidgety movements were observed in infants between 3 and 6 months. Spastic (16.9%) or dystonic (one case) movements and postures were observed. Acquisition of motor and behavioral milestones was markedly delayed in all cases. None of the infants examined after 6 months of age were able to hold a stable sitting position for more than a few seconds, Persistent and repetitive tongue thrusting was particularly evident even in the absence of external stimuli. Strabismus was observed in 10 cases (12%) and nystagmus in four cases (4.8%).

## 3.5 | Brain imaging

Eighty two infants had cranial CT, five had brain MRI. Some combination of characteristic abnormalities including multiple calcifications (92.8%), poor and abnormal gyral patterns (36.1%), ventriculomegaly and prominent extraaxial spaces (72.3%) and/or hypoplasia of the brainstem and cerebellum (16.9%) suggested prenatal infection consistent with ZIKV in all patients. There was in all cases a marked decrease in gray and white matter volumes, often with thinning or absence of the corpus callosum, and hypoplasia of the ventral pons (Table 5 and Figure 8).

No significant associations were found between the frequencies of dysmorphic, neurologic and abnormal neuroimaging features among the three groups of Z scores of HC.

## 3.6 | Viral serologies and viral detection

ZIKV specific IgM in CSF was determined in 14 infants. The antibodies were positive in 12 infants and negative in two. Specific

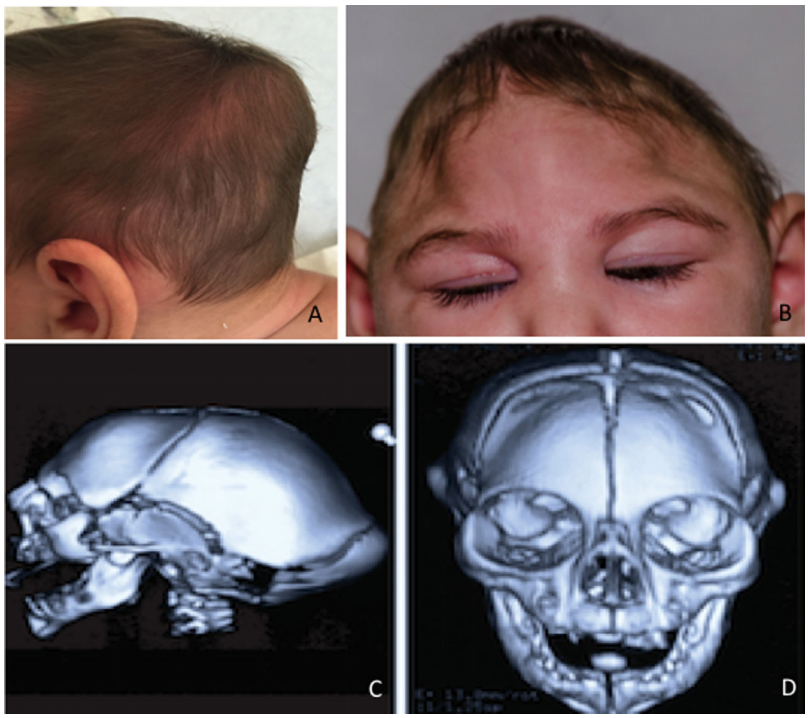


**FIGURE 3** The occipital prominence can be pronounced and evident on external inspection (A) and represents the parietal-occipital junction with a very hypoplastic occipital bone on reconstructed CT image (C). A frontal midline bulge is apparent due to significant depression of the lateral aspects on the frontal bone (B), which appear more depressed than the parietal bones along with obvious supratemporal depression on CT (C and D). The vertical dimension of the cranium is reduced and the parietal vault is narrow (B and D). [Color figure can be viewed at wileyonlinelibrary.com]

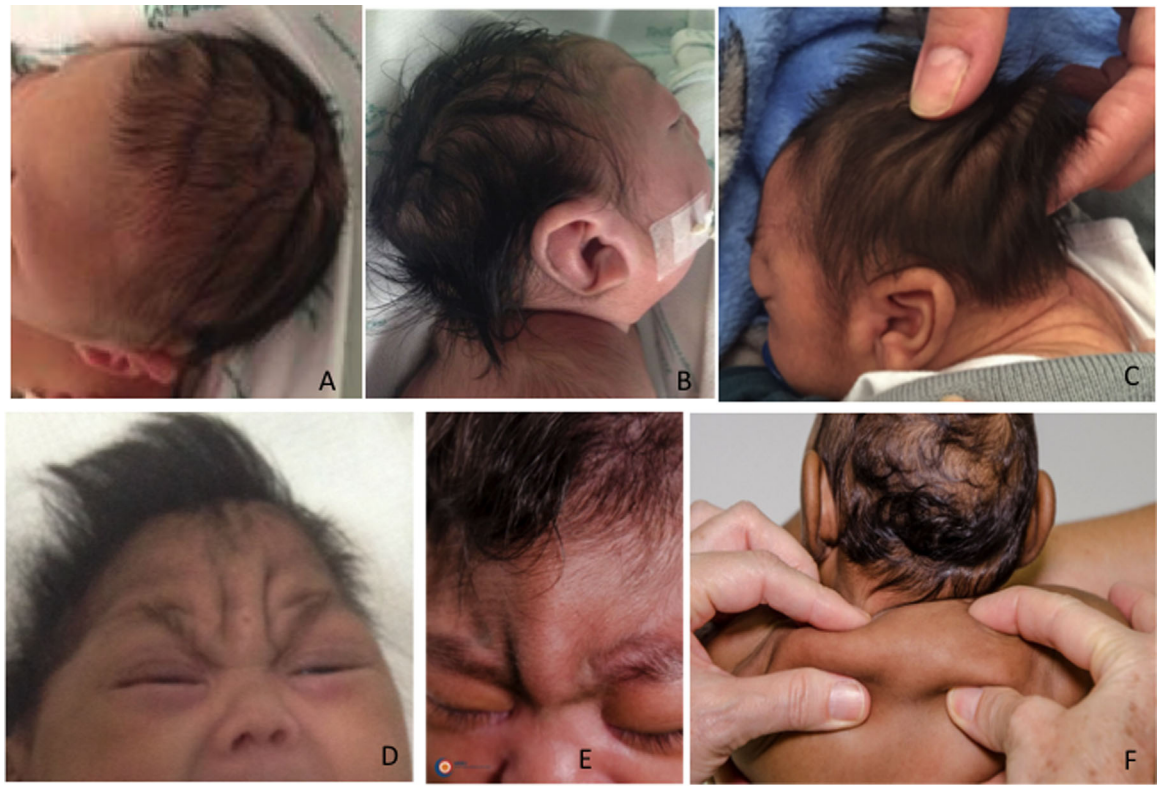


**FIGURE 4** Redundant skin of the scalp creating transverse folds, that is,"cutis rugata" (A), or more cerebriform patterns, that is, "cutis gyrata" (B). In other cases, redundant skin is obvious only over the occipital region (C), or the glabellar region, where it can create several furrows (D) or a bulging single fold, with a crease above the nose. Epicanthal folds, and full periorbital tissues (E). The excess skin can be observed in the back as well (F). [Color figure can be viewed at wileyonlinelibrary.com]

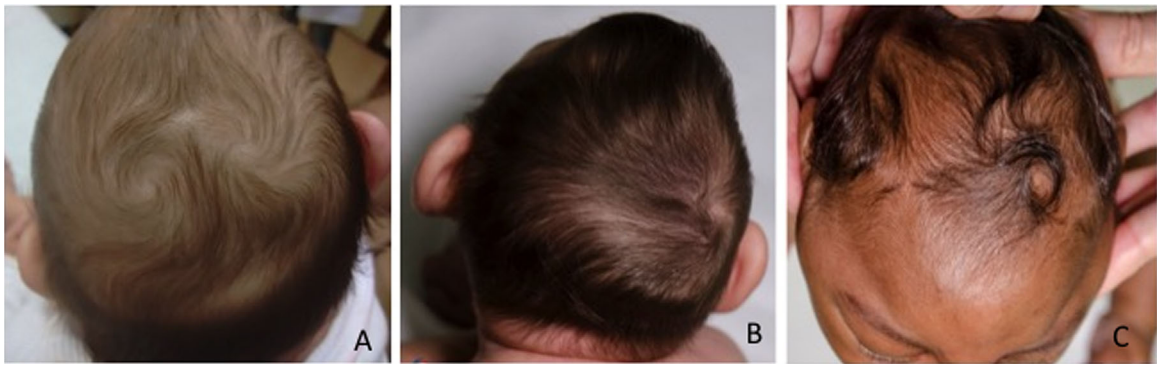


**FIGURE 5** Several infants had abnormal hair patterns such as double hair whorls at the vertex (A), an excessively lateralized posterior whorl (B), or frontal upsweep and frontal hair whorl (C). [Color figure can be viewed at wileyonlinelibrary.com]

viral PCR were negative in all newborns and infants in whom this test was performed. The phenotype of the 12 antibody positive cases ranged from severe skin and skull features to a milder and less obvious phenotype exhibiting a similar spectrum to that of the rest of the group. Three cases with contractures had confirmed IgM in CSF. Also, the two cases with negative IgM had findings consistent with the rest of the group. Cases with positive and negative IgM are highlighted in Supplemental Table S6. The frequencies of findings in

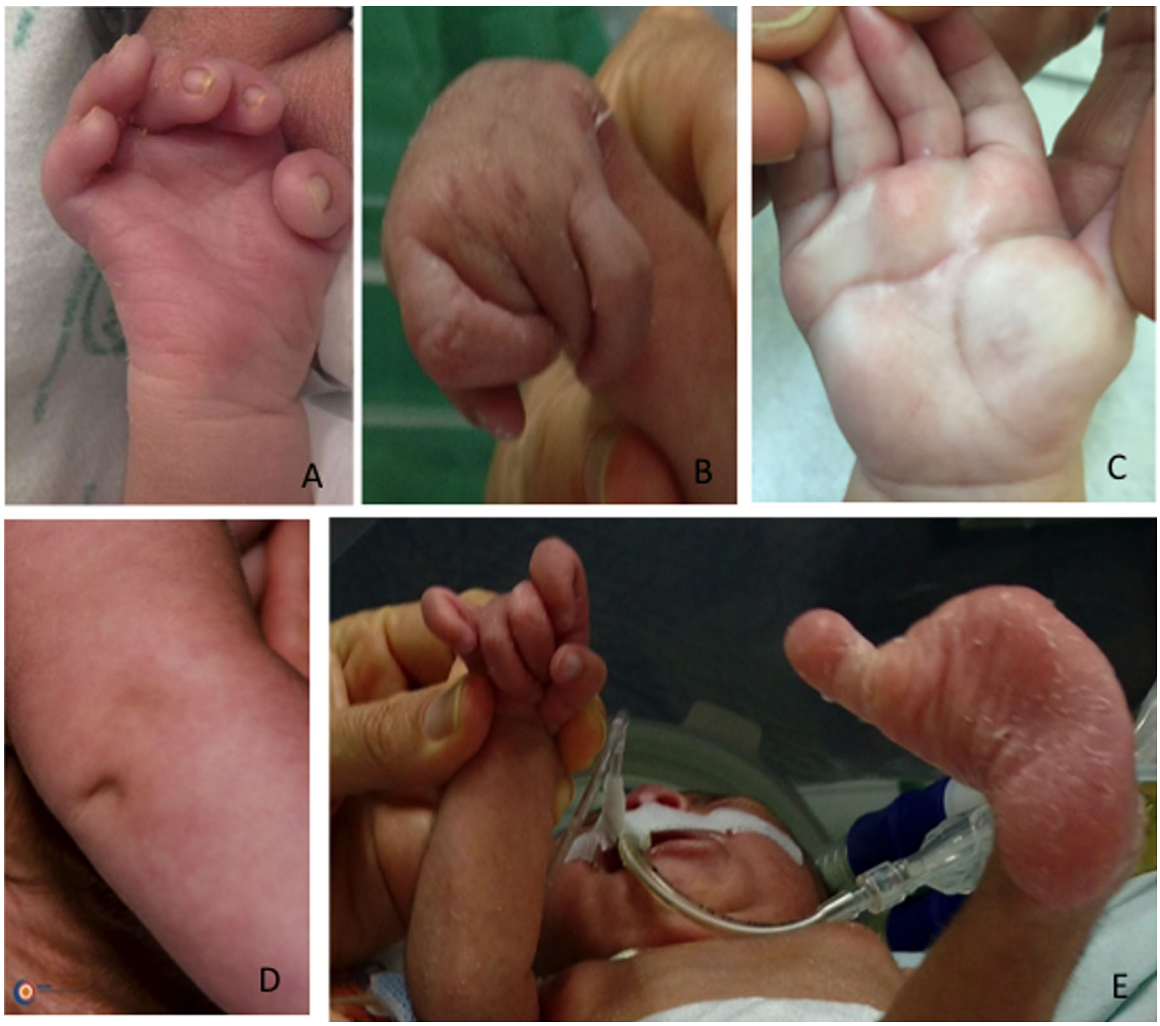


**FIGURE 6** The most common observed features of immobility are distal contractures or dimples. Finger contractures or camptodactyly (A), wrist contractures (B). The palm shows an abnormal and deep single palmar crease, and the fingers have contractures, yet show faint flexion creases at the interphalangeal joints (C). Deep dimple at the elbow (D). Child with distal contractures in hands and club feet, and who requires a nasogastric tube for feeding (E). [Color figure can be viewed at wileyonlinelibrary.com]

**TABLE 4** Main neurologic findings

| Findings | *N* = 83 | % | IgM+ CSF (*N* = 12) |
|---|---|---|---|
| Irritability | 30 | 36.1 | 2 |
| Abnormal pattern of cry | 19 | 22.9 | 3 |
| Hyperexcitability | 19 | 22.9 | 2 |
| Distal tremors | 15 | 18.1 | 0 |
| Hypertonia | 62 | 74.7 | 12 |
| Trunk hyperextension or hyperflexion | 24 | 27.7 | 0 |
| Spasticity | 14 | 16.9 | 4 |
| Increased deep tendon reflexes | 17 | 20.5 | 1 |
| Persistent primitive responses | 8 | 9.6 | 0 |
| Clenched fists | 17 | 20.5 | 5 |
| Strabismus | 10 | 12.0 | 2 |
| Nystagmus | 4 | 4.8 | 1 |

the 12 cases with positive IgM in CSF are included in Tables 2–5, for comparison with the total group.

### 3.7 | Health complications

The great majority of the infants were born healthy with no indication of altered function of any organ or system other than the nervous system, and experienced normal feeding and growth. Some infants, particularly, but not only, those with arthrogryposis (9.6%), have had significant feeding difficulties and gastroesophageal reflux with aspiration, and a few have had serious respiratory complications. Some have been candidates for tracheostomy and G tube placement, procedures that have naturally elicited bioethical discussion among their health care providers and the children's families. In some cases, feeding difficulties appeared several weeks or months after birth. Seizures developed, particularly at 3–6 months of age in several infants. Abnormal EEG's have been recorded in several cases, both with baseline alterations and epileptic seizure activity. The details on the neurologic follow-up of these infants will be published elsewhere.

## 4 | DISCUSSION

The suspicion of a causal relationship between microcephaly and ZIKV, and the preliminary evidence of a specific clinical phenotype beyond isolated microcephaly in a study of 35 infants by Schuller-Faccini et al, prompted us to study in greater detail the phenotypic spectrum of this newly recognized pattern of disruption, as well as to speculate regarding the underlying developmental pathogenesis (PAHO, 2015; Schuler-Faccini, Ribeiro, et al., 2016; Schuler-Faccini, Sanseverino, et al., 2016). Assuming the current evidence as sufficient for causality, the phenotypes described in these 83 infants most likely result from ZIKV prenatal infection of the embryo and fetus (Brasil, Pereira, Moreira, et al., 2016; de Araújo et al., 2016; França et al., 2016;

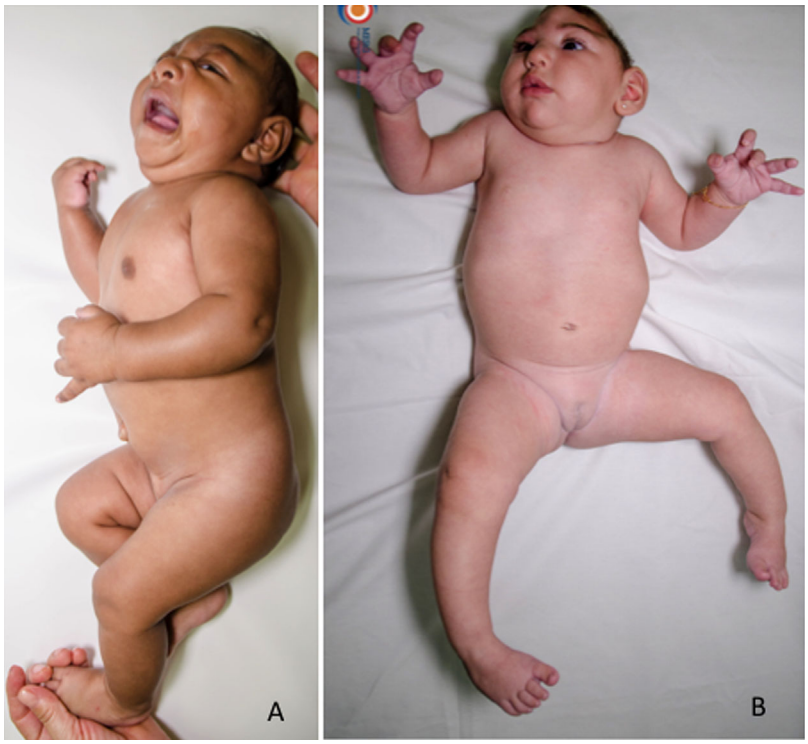


**FIGURE 7** Two infants with abnormal neurological features. Hypertonic trunk extensor posture (A), and distal tremors and spasticity of lower limbs (B). [Color figure can be viewed at wileyonlinelibrary.com]

**TABLE 5** Main findings on brain imaging

| Findings | *N* = 83 | % | IgM+ CSF (*N* = 12) |
|---|---|---|---|
| Calcifications | 77 | 92.8 | 12 |
| Cortical-subcortical | 71 | 85.5 | 11 |
| Basal ganglia | 21 | 25.3 | 0 |
| Periventricular | 13 | 15.7 | 1 |
| Cortico-subcortical atrophy | 34 | 41.0 | 2 |
| Abnormal gyral pattern | 30 | 36.1 | 0 |
| Polymicrogyria | 20 | 24.1 | 0 |
| Ventricular dilatation and/or increased extra-axial fluid | 60 | 72.3 | 8 |
| Dysmorphic ventricles | 14 | 16.9 | 0 |
| Vermis hypoplasia | 14 | 16.9 | 2 |
| Cerebellar atrophy | 12 | 14.5 | 1 |
| Corpus callosum agenesis/ dysgenesis | 9 | 10.8 | 1 |

Honein et al., 2017; Rasmussen, Jamieson, Honein, & Petersen, 2016; Schuler-Faccini, Sanseverino et al., 2016). This study provides detailed insight into the range of the phenotypes observed in these infants.

## 4.1 | Main conclusions

The present study on the phenotype of these 83 infants has led to three main conclusions:

1. The phenotype resulting from ZIKV congenital infection is typically severe, and will significantly impact patients' future neurologic development.
2. This phenotype is frequently recognizable in infancy and can be defined as a disruptive sequence. That is, the teratogen ZIKV disrupts the development of the brain, producing a sequence of secondary anomalies that we term the "Embryo-Fetal Brain Disruptive Sequence by the ZIKV" (EFBDS-ZIKV).
3. There is a clinical range in terms of both the overall type and the severity of findings. All cases had significant cerebral lesions, but the spectrum ranged from absent/mild/moderate microcephaly without distinctive dysmorphic features to a more obvious phenotype of severe microcephaly frequently associated with the appearance of collapse of the skull and skin redundancy, sometimes with arthrogryposis. Skull abnormalities were present in 69.7%, redundant skin was present in 67.4%, but these signs were often subtle. The most severe phenotype of the previously described Fetal Brain Disruption Sequence (FBDS) (Corona-Rivera et al., 2001; Moore, Weaver, & Bull, 1990; Russell, Weaver, Bull, & Weinbaum, 1984) was identified only in a minority of infants, and was more evident at birth. The range of severity of neurologic abnormalities is broad as well. The timing of maternal infection may explain some of the observed variability (Soares de Souza et al., 2016). Early infection may determine a pattern of severe microcephaly with abnormal hair patterning. More frequently, maternal infection presumed to occur in late first and early second trimesters appears to lead to the appearance of collapse of the skull and redundant skin. It is suggested that later infection leads to a lesser decrease in HC, with a less pronounced cranial and scalp phenotypes and milder neurologic impact.

## 4.2 | Limitations of the study

The main limitation of this study is the absence of confirmed ZIKV in all cases. When performed, specific PCR for ZIKV in newborn samples (blood, CSF) has been negative at birth in live-born cases. The diagnosis of ZIKV maternal infection via RT-PCR of serum for detection of ZIKV RNA is positive only for a brief window of time, 5 days after the onset of clinical symptoms. In pregnancies with evidence of fetal infection, ZIKV RT-PCR in the mother's serum can persist as long as 100 days, suggesting that persistent maternal viremia may occur as a consequence of viral replication in the fetus or placenta, where viremia has been proven to persist several weeks (Calvet et al.,

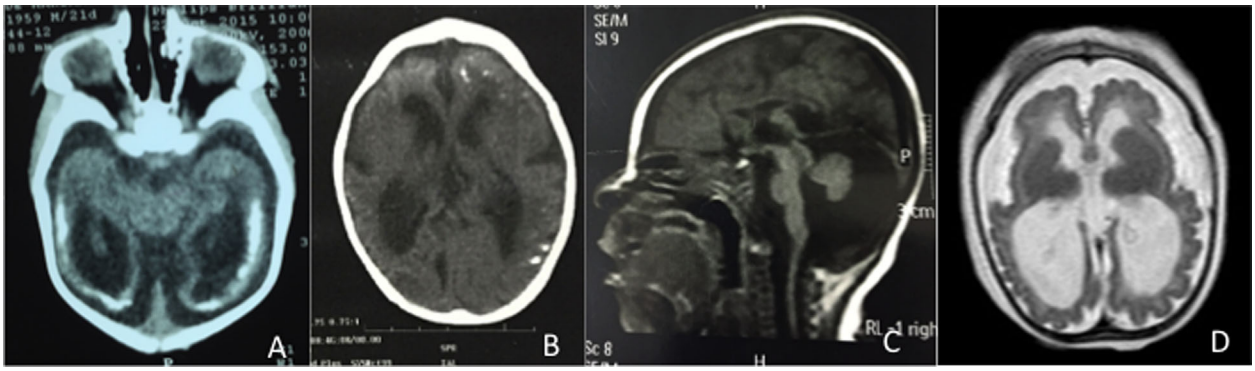


**FIGURE 8** CT scans of different patients identified extensive cortical-subcortical calcifications with an almost band-like pattern (A), or more discrete calcifications at the cortical margins (B), as well as increased ventricular and extra-axial fluid (A and B) and ventricular asymmetry and dysmorphia on coronal images. Sagittal image identifying a thin and incomplete corpus callosum, as well as increased extra-axial fluid with a cystic dilatation of the posterior fossa (C). T2 sequence of brain MRI showing subarachnoid space dilation, ex-vacuo ventricular dilation, and a pattern of simplification of the cerebral cortex with polymicrogyria (D). [Color figure can be viewed at wileyonlinelibrary.com]

2016; Carvalho, Cordeiro, et al., 2016; Suy et al., 2016). ZIKV specific IgM is present in the infant's serum but its presence in CSF has become the gold standard for proving CNS infection in affected newborns (Cordeiro et al., 2016), since maternal IgM does not cross the placental barrier and fetal serum IgM does not freely cross the blood-brain barrier. Although ZIKV specific IgM in CSF was only available in 14 cases in this study, and positive in 12, infants without positive specific IgM had brain imaging findings and clinical phenotypes similar to those with confirmation. In the two cases in which IgM titers were negative in CSF, neuroimaging findings and the clinical phenotype were consistent with the rest of the group. No current evidence has established the sensitivity of this assay. The brain imaging findings, used as the inclusion criteria, appear particularly specific to ZIKV infection (Brasil, Pereira, Moreira, et al., 2016; Cavalheiro et al., 2016; Guillemette-Artur et al., 2016; Hazin et al., 2016; Soares de Oliveira-Szejnfeld et al., 2016). Congenital CMV infection remains the most likely alternate diagnosis, but was ruled out in 71% of infants. However, the overall severity of the findings and, particularly, the widespread distribution of predominantly subcortical calcifications in cases of ZIKV, in contrast with the periventricular distribution in CMV, make congenital CMV a less likely explanation in the cohort described here (Alarcon et al., 2013; Averill, Kandula, Akyol, & Epelman, 2015; Capretti et al., 2014). Most infants had available normal TORCH serologies (71.1%), which ruled out other congenital infections included in this panel.

The date of suspected maternal infection was unclear in most mothers, which led to an exposure estimation based on months of gestation as opposed to weeks. In addition, the co-occurrence in Northeast Brazil of other rash-causing arboviral infections (Dengue and Chikungunya) is also challenging (Chang, Ortiz, Ansari, & Gershwin, 2016). Further, a high percentage of asymptomatic maternal infections has been documented in most studies and was above 20% in this series. These factors may explain the study's inability to show statistically significant correlations between gestational age of the maternal rash and the variable phenotypes observed. It has been shown that ZIKV infection at any time of gestation up to 39 weeks can affect the fetus (Brasil, Pereira, Moreira, et al., 2016).

It is important to recognize that, because of the experience acquired in evaluating the initial patients, all patients were not evaluated using the same protocol. This may have led to under-recognition of some features in earlier examined infants. In our opinion, this does not alter the qualitative evaluation of the overall findings. The expertise of clinical geneticists and pediatric neurologists in the recognition of many subtle features enhance the descriptive detail of previous studies, including case reports and case series (Besnard et al., 2016; Culjat et al., 2016; França et al., 2016).

We also believe that our study is biased toward children at the most severe end of the phenotypic range. A review of multiple previous reports has described the most apparent and severe phenotypes (Moore et al., 2016). This study emphasizes that cases without microcephaly at birth may have later emerging microcephaly or developmental delays, as documented by contributors to this study (Van der Linden, Pessoa, Dobyns, Barkovich, & Júnior, 2016). Less severe phenotypes, which may go initially unrecognized are emerging in clinical reports particularly after maternal infection in the third trimester of pregnancy (Soares de Souza et al., 2016). A recent report of a large prospective cohort of 117 proven ZIKV exposed pregnancies reported adverse outcomes in 46% of fetuses or live-born infants, but identified microcephaly in only four infants (3.4% of the exposed live-born infants). This new evidence highlights the fact that our initial criterion for ascertainment of infants with a HC ≤33 cm biased our study toward the more severely affected cases.

Finally, our follow-up data is still insufficient to delineate the postnatal history of the disorder, but our preliminary insight into the health complications in these infants may lead to improved surveillance, recognition, and treatment of the most common medical problems. Larger datasets have proven that fetal and neonatal mortality rates are increased (França et al., 2016). Impaired somatic and head growth and has been observed in this study, and reported in others (Moura da Silva et al., 2016). Referral to the CDC recommendations for follow up and management of infants with congenital ZIKV infection is appropriate until further evidence becomes available (Russell et al., 2016).

## 4.3 | The significance of the findings

The observed dysmorphic and neurologic phenotypes merit interpretation, based both on knowledge of embryonic and fetal development and on the evidence generated in the literature since the onset of this epidemic.

### 4.3.1 | Prenatal and postnatal growth

Prenatal growth in length and weight are affected in our series of 83 live newborns. One obvious reason for a possible decrease in length and weight is the significant decrease in the size and weight of the cranium and brain in these infants, as evidenced by significant correlation among measures of HC and BL and BW. However, it is important to recognize that past attempts to correlate measures of HC and somatic growth in healthy infants have been problematic (Illingworth, 1965; Nishi et al., 1992). Clearly, the difficulties in estimating the decrease in volumes and weights of the cranium and brain in these infants with standard measures of HC contribute to the difficulty in determining whether somatic growth is in fact independently affected by the ZIKV prenatal infection. However, some features in these infants suggest that growth deficiency is a feature of this condition. For example, the observed redundant skin folds over the body may point to an arrest or a decreased rate in somatic growth some time during pregnancy. Hydrops including subcutaneous edema has been reported in some affected fetuses and could also lead to redundant skin (Sarno et al., 2016). Recent prenatal studies confirm IUGR can occur and can be severe (Melo et al., 2016). ZIKV infection of the placenta and the fetal membranes has been demonstrated in multiple reported cases of abortion and stillbirth. ZIKV prenatally infected mice have IUGR indicating that placental infection leading to placental inflammation and dysfunction has an impact on fetal growth and viability (Brasil, Pereira, Raja Gabaglia, et al., 2016; Cugola et al., 2016; Driggers et al., 2016; Sarno et al., 2016; van der Eijk et al., 2016). In the recent prospective study from Rio de Janeiro, only 8.6% of infants were reported as small for gestational age (<−1.28 SD), versus

5.3% in the non-exposed groups. Median BW did not differ significantly among the exposed and non-exposed groups. Transient decelerations in fetal growth with later catch-up in pregnancy were observed in several cases (Brasil, Pereira, Moreira, et al., 2016).

Prematurity in our series was increased over the reported rate in Brazil, but was not extreme, in agreement with other studies (Brasil, Pereira, Moreira, et al., 2016; Leal et al., 2016). In other congenital infections such as CMV, also approximately one-third of affected live born infants have a gestational age less than 37 weeks (Alarcon et al., 2013).

### 4.3.2 | Microcephaly, cranial shape, redundant scalp, and hair patterning

Microcephaly was the main observable feature in affected infants, in part due to our inclusion criteria. The findings are consistent with other larger epidemiologic reviews, with one-third of cases presenting without microcephaly at birth (Microcephaly Epidemic Research Group, 2016; Schuler-Faccini, Ribeiro, et al., 2016), but much higher than the 3.4% in the recent study in Rio (Brasil, Pereira, Moreira, et al., 2016). Due to the abnormal skull morphology, particularly the occipital prominence, the ability to measure HC was problematic, which may offer an explanation for the discordant rates of microcephaly among different studies. Moreover, HC does not appear to be a good measure of brain size in these infants. Although the shape of the cranium is variable among cases, there is almost always a subjective decrease in the vertical size of the cranium in addition to the reduction of the occipito-frontal circumference. This may explain why we did not demonstrate statistically significant phenotypic differences in the dysmorphic and neurologic variables among the three ranges of HC in this study.

The overall shape of the cranial vault, including the overlapping and early ridged sutures, often with closed fontanels, and the abnormal bony prominences in the frontal, temporal, and occipital areas, are the most characteristic features of the skull of these infants and merit speculation. The bones of the membranous neurocranium (frontal, parietals, the squamous portion of the temporal bones, and the occipital bones) are all subjected to disrupted growth and deformation, due to the decreased and abnormal growth of the underlying brain, or to an actual decrease in brain size. In contrast, the bones of the cranial base, which undergo endochondral ossification, and are attached to the viscerocranial facial bones (Sadler, 2015), appear unaffected, leading to normal facial size and structure.

In most of these infants, the frontal bone is depressed on both sides; deficiency of the squamous portion of the temporal bones and the parietal bones create supratemporal depressions above the apparently preserved volume of the lower portion of the temporal bones. Posteriorly, the occipital bone appears to collapse and wrinkle in its vertical dimension creating the occipital prominence (Figure 4). As the overlying head shape reflects the underlying brain, these shapes may reflect those areas of the developing brain that are most affected.

The scalp, particularly at the forehead and nuchal areas, is loose and redundant, creating abnormal configurations and folds where the cranium is most deficient and misshapen (Figure 3). This redundancy appears to be the mechanism leading to the epicanthal folds and the full periorbital tissues seen in some patients.

Our current knowledge does not allow us to answer the question of whether the abnormal shape of the bones making up the calvarium and the redundant scalp are the consequence of an acute decrease in brain size related to a sudden decrease in intracranial pressure at some point in pregnancy, or rather that the collapsed appearance of the bones and the disproportionate growth of the skin are slow and progressive.

In most infants affected by genetic conditions associated with microcephaly, these alterations in bone and skin described in ZIKV infants are not seen. For example, in babies with severe primary microcephaly, the surface of the skull is smooth and the intracranial volume is globally decreased, with posterior sloping of the forehead, and normally tight skin over the cranial vault (Verloes, Drunat, Gressens, & Passemard, 1993). In those cases, the brain is programmed to be small, and appears to lead to a synchronic and proportionate development of the overlying structures. However, some abnormal shapes of the skull are seen in other genetic disorders. A prominent metopic ridge causing trigonocephaly or a narrow forehead is often seen in genetic conditions with neurologic involvement with or without microcephaly. Similarly, a prominent occiput is seen in conditions like trisomy 18 and other conditions that include smaller brain size (Jones, Jones, & Del Campo, 2013). In those cases, the abnormal shapes of the skull may reflect decreased growth of specific brain regions. The presence of redundant skin may also reflect this. For example, in the Miller Dieker syndrome (Jones et al., 1980), caused by a microdeletion of chromosome 17p13.3 (Stratton, Dobyns, Airhart, & Ledbetter, 1984) involving LIS1 and other genes leading to severe lissencephaly, bulging vertical furrows of redundant skin can be seen over the glabella and forehead, reflecting a deficiency of frontal brain development, without any additional evidence of collapse of the cranium. These observations suggest that some of the features seen in this disorder can be observed, to a lesser degree, in infants with microcephaly due to other causes without an actual sudden decrease in brain volume causing an acute collapse of the cranial vault.

Interestingly, most children in this ZIKV group have normal hair patterning. The patterns of hair of the scalp depend on growth of the underlying brain. Normally, the scalp hair sweeps down in the frontal area, and there is a single posterior hair whorl. Any deviation from this pattern is infrequent and merits consideration of an underlying brain defect (Furdon and Clark, 2003). These patterns are established before 16 weeks of gestation, and depend on brain growth from 10 to 16 weeks (Smith and Gong, 1973). According to our observation, the period of pregnancy when this phenotype appears in the fetus is usually later than 16 weeks. In agreement with this observation, prenatal imaging studies have identified abnormal brains and skull shapes of infected fetuses in the second half of the pregnancy (Brasil, Pereira, Raja Gabaglia, et al., 2016; Carvalho, Cordeiro, et al., 2016). We observed abnormal hair patterns in five cases (Figure 5), which suggests that, in those cases, the onset of events leading to these dysmorphic features must have occurred prior to 16 weeks gestation. Those five cases with abnormal hair patterns have severe microcephaly and neurologic impairment but only had mild features, possibly suggesting collapse of the skull. When recalled, gestational age of maternal infection was in the first trimester in these cases. They may

represent a phenotype consistent with earlier infection, affecting brain growth at the end of the embryonic period.

#### 4.3.3 | Joint contractures

The third set of important features involves joint abnormalities. In normal fetal development, joint development is dependent on normal fetal activity. In the case of ZIKV infection, decreased fetal activity results from disruption in brain development. Mild cutaneous features at the joints, such as multiple and large dimples or creases, foot malpositions and hand contractures, were seen frequently (Figure 5). A smaller proportion of cases (10%) had definite interruption of fetal movement leading to generalized arthrogryposis, as noted in other studies (Moura da Silva et al., 2016; Sarno et al., 2016). Cutaneous dimples at the joints are known to occur when movements are decreased in arthrogryposis syndromes, leading to sustained positioning that favors the adherence of the skin to the bone (Kumar, Kanojia, & Saili, 2014). Even when mobility is normal at birth, dimples and abnormal foot and hand positions appear to reflect periods of decreased movement in utero. In most cases of genetically determined congenital arthrogryposis, wrist, and finger contractures determine abnormal palm and finger creases. The digital creases are present in the skin before 9–10 weeks of gestation (Kimura and Kitagawa, 1986). Palmar creases appear later, before 13 weeks (Stevens, Carey, Shah, & Bagley, 1988). In most cases of camptodactyly in these infants, faint creases were seen even in immobile joints, suggesting immobility occurred after normal movement had started at 9 weeks. (Figure 5). In at least two cases the presence of normal interphalangeal creases and abnormal palmar creases may date the onset of immobility to between 9 and 13 weeks. Also, tight and webbed skin over the joints or pterygia in many conditions with arthrogyposis suggest fetal movement never occurred. In cases of arthrogryposis identified in this study, no pterygia were found, indicating the onset of immobility must have occurred after the onset of fetal movement. Finally, the deep palmar creases seen in many infants with and without contractures suggest sustained spastic clenched positions of the hands in utero. When comparing fetuses with and without contractures, a specific gestational age of recalled maternal infection at which arthrogryposis occurred could not be identified in this study. In general, our observations indicate that onset of immobility occurred in the second trimester. Two other features may reflect abnormal intrauterine movements. Micrognathia was more severe in fetuses with arthrogryposis but milder degrees were seen in many infants without arthrogryposis. Also, the broad alveolar ridges observed may represent decreased tongue movements during some time in pregnancy (Hanson, Smith, & Cohen, 1976). Interestingly, the absence of the lingual frenulum is characteristic of the Ehlers Danlos syndrome (EDS) (De Felice, Toti, Di Maggio, Parrini, & Bagnoli, 2001; MacHet et al., 2010); in EDS, this feature is due to tissue hyperelasticity. In ZIKV congenital infection, the recurrent and vigorous tongue thrusting movements in many infants after birth may explain why this feature developed prenatally (Figure 2). The specific clinical presentations of arthrogryposis in infants with ZIKV congenital infection have also been described in detail and discussed in other studies (Sarno et al., 2016; van der Linden et al., 2016).

The significant reduction in cerebral grey and white matters and the evident reduction of the ventral prominence of the pons on brain imaging suggest that a central cause of the immobility leads to arthrogryposis in most cases. Contractures may be present only when corticospinal tract thinning is very significant, or when damage may directly affect the spinal cord, but this remains to be determined by further neuroimaging analysis of infants and pathology studies of deceased fetuses. A central origin of the arthrogryposis would also be in agreement with the overall abnormalities in brain function, with hypertonia and spasticity being present in most infants without contractures. There may be a pathogenetic continuum between spasticity and arthrogryposis dependent on the severity and/or timing of the brain disruption. Although a single case in the sample had an MRI of the spinal cord, which was normal, the spinal cord has been described as thinned in other studies of affected infants (van der Linden et al., 2016).

#### 4.3.4 | Neurologic phenotype

This study provides a description of the major anomalies in neurologic functions in these infants. In agreement with findings on neuroimaging in this series and others and with the pathology of the CNS in other studies, the neurologic consequences of ZIKV congenital infection are devastating, sicne all major cerebral functions are compromised (Martines et al., 2016; Melo et al., 2016). With the necessary limitations imposed by the exam of newborns and very young infants, cognition, behavior, motor, and sensory functions all appear to be affected. The abnormal neurobehavior and sensory processing, and the more objective motor deficits, characterized by alteration of motor activity (tone, posture, and motility), all indicate severe global damage. Furthermore, brain images with significant reductions in cortical and subcortical volumes, extensive, and multiple calcifications and abnormal gyral patterns are all in agreement with the severity of the clinical phenotype observed. Recently abnormal EEG have been reported in the majority of affected infants, regardless of the presence of clinical seizures (Carvalho et al., 2017).

#### 4.3.5 | Ocular findings

Finally, ocular findings observed in patients in the present series are similar to findings previously observed and will be reported in detail elsewhere (de Paula Freitas et al., 2016; Ventura, Maia, Bravo-Filho, et al., 2016, Ventura, Maia, Travassos, et al., 2016; Ventura, Maia, Ventura, et al., 2016). In some cases poor visual function was evident on exam, with poor fixation and tracking. Also, some infants had microphthalmia, strabismus, or obvious nystagmus. The eye is an additional target of the ZIKV infection, in part related to cerebral damage, but also due to specific involvement of the intraocular structures, particularly the retina.

Data on hearing deficits were not specifically assessed in this study. Others have reported sensorineural hearing loss in a few cases (Carvalho, Ferreira, et al., 2016; Microcephaly Epidemic Research Group, 2016).

## 5 | THE FBDS

In 1984, a similar clinical pattern of sporadic congenital defects was described in three cases as the FBDS (Russell et al., 1984). The authors hypothesized that in utero brain disruption or destruction resulting from prenatal viral infection, vascular insult, or hyperthermia, after the 12th week of pregnancy, followed by diminished intracranial pressure, could lead to collapse of the fetal skull. FBDS has been rarely described, often with calcifications and very similar brain imaging findings to those we report here, and has been usually interpreted as a sporadic condition with poor prognosis and low recurrence risk (Bonnemann & Meinecke, 2000; Corona-Rivera et al., 2001; Hughes, 1986; Moore et al., 1990; Villó, Beceiro, Cebrero, & de Frias, 2001). All of these reports suggest that a disruptive-destructive process occurs relatively acutely in a normally developing brain. Interestingly, similar phenotypes have been reported in cases with recurrence in siblings, thought to have genetic causes with an autosomal recessive pattern of inheritance, sometimes due to known causal genes for microcephaly without the FBDS phenotype (Alexander, Tauro, & Bankier, 1995; Paciorkowski et al., 2013; Schram et al., 2004). The dysmorphic phenotype in those cases is similar in terms of cranial and scalp anomalies, but is proposed to occur by an arrest in brain development rather than a destruction, at least in some cases (Abdel-Salam et al., 2015). Other genetic FBDS phenotypes such as Hemorrhagic destruction of the brain, subependymal calcification, and cataracts (MIM 613730), due to *JAM3* mutations, and mutations in *OCLN2* causing band-like calcification with simplified gyration and polymicrogyria (MIM 251290) appear to lead to a destructive hemorrhagic process in the brain (Abdel-Salam, Zaki, Saleem, & Gaber, 2008; Mochida et al., 2010). These examples are genetic alterations leading to disruption in development after a period of likely normal neural tissue formation. None of these reported cases have been associated with arthrogryposis and the neurologic findings on exam, when reported, were significantly different from those we identified in ZIKV prenatally infected infants. Therefore, even though the visible cranial phenotype of the FBDS appears to be similar, ZIKV appears to disrupt brain development in a specific manner. The details of these processes are being studied in different model cells, organoids and live organisms (Cugola et al., 2016; Dang et al., 2016; Dudley et al., 2016; Goodfellow et al., 2016).

Unlike some other congenital viral infections able to affect multiple organs and tissues, ZIKV appears to have tropism for a limited number of tissues, and demonstrates particular neurotropism (Cordeiro et al., 2016; Hazin et al., 2016; Mlakar et al., 2016; Tang et al., 2016). Damage by the ZIKV to the nervous system was initially observed in experiments involving the intracerebral inoculation of newborn mice (Bell, Field, & Narang, 1971). Similar lesions in the neuronal tissues were recently observed in the human fetus and in murine models (Cugola et al., 2016; de Fatima Vasco Aragao et al., 2016; Driggers et al., 2016; Huang, Abraham, Shim, Choe, & Page, 2016; Li et al., 2016; Mlakar et al., 2016). Recent work in ZIKV infected brain organoids and mice suggest that infection of neuronal progenitors causes activation of specific receptors involved in innate immunity, and activates specific genetic pathways that change the fate of neural cells (Dang et al., 2016; Zhang et al., 2016). Apoptosis and autophagy of these neural progenitors appear to underlie the severe disruption in neural development by the ZIKV, and the period of maximum brain growth appears particularly susceptible to effects of the infection (Huang et al., 2016). The process from the initial brain infection to widespread neuronal death may be slow, as reflected by the detection of brain abnormalities on prenatal ultrasound many weeks after the onset of maternal infection (Brasil, Pereira, Raja Gabaglia, et al., 2016). The sequence of events affecting brain growth, structure and function during this long period of 10 weeks or more is still unknown. This study suggests that many of the dysmorphic features observed occur in the second trimester of pregnancy. The presence of abnormal palmar creases and hair patterning indicates fetal immobility and suggests that abnormal growth of the brain may be occurring earlier in pregnancy, in the late embryonic period in some patients.

## 6 | IMPLICATIONS OF THIS STUDY FOR CLINICAL CARE AND FUTURE RESEARCH

As clinicians and clinical researchers, we need to improve our ability to define what contributes to the variable severities of ZIKV brain damage and other phenotypic manifestations. The fact that we failed to identify significant associations between the recalled age of maternal infection and phenotypic expression in patients suggest that improved documentation of the onset of maternal infection will be helpful to better address this question. Routine viral and immunologic studies during pregnancy in affected areas are necessary to determine the rate of birth defects in exposed fetuses and newborns, as well as the impact of infection at different times in pregnancy. Recent studies identify very different outcomes in ZIKV infected pregnancies. The study in Rio identifies 46% of affected fetuses and live-born infants after infection in all three trimesters of pregnancy, whereas in a study of 442 pregnancies in the United States, only 6% had birth defects, and only after infection in the first trimester (Brasil, Pereira, Moreira, et al., 2016; Honein et al., 2017).

We pointed out that measurements of HC are difficult and imprecise in these patients and likely inadequately represent brain volume. Better external measures of intracranial volume should be proposed, given the abnormal shapes of the skull in these patients. Possible modalities include 3D imaging of the face and reconstructed 3D scanning of the head. Where advanced neuroimaging is available, MRI with segmentation of brain volumes (Anbeek et al., 2013) may be better able to correlate specific measures with neurologic outcome.

In order to detect prenatal infection of the fetal brain as early as possible, improved identification of cranial and brain lesions should be sought utilizing 3D ultrasound and fetal MRI (Rochelson, Vohra, Krantz, & Macri, 2006). Our observations suggest that closer follow up of the rates of brain growth and more suitable measurements of the fetal head will aid in early prenatal detection The qualitative observation and quantification of fetal movements with 4D ultrasound (Kurjak et al., 2008) may also aid in early prenatal detection of functional neurologic damage to the fetus. This study also indicates that, detailed physical and neurologic evaluations of the affected infants by expert clinicians, and objective measures and scales of severity for both the dymorphologic

and neurologic phenotypes, will be essential for the assessment of outcome and for the identification of prognostic factors.

## ACKNOWLEDGMENTS

We thank all the families for their support of this study. We also thank the Brazilian Ministry of Health, Pernambuco State Health Department, and Pan American Health Organization, and Centro de Pesquisas Aggeu Magalhães/Microcephaly Epidemic Study Group, and AACD from Pernambuco for their support. The authors received partial support from the Conselho Nacional de Desenvolvimento Científico e Tecnológico (scholarship 306489/2010-4 to C.M.T.M.), and from the Brazilian Society of Medical Genetics.

## REFERENCES

Abdel-Salam, G. M., Zaki, M. S., Saleem, S. N., & Gaber, K. R. (2008). Microcephaly, malformation of brain development and intracranial calcification in sibs: Pseudo-torch or a new syndrome. *American Journal of Medical Genetics Part A*, *146A*, 2929–2936.

Abdel-Salam, G. M., Abdel-Hamid, M. S., El-Khayat, H. A., Eid, O. M., Saba, S., Farag, M. K., . . . Gaber, K. R. (2015). Fetal brain disruption sequence versus fetal brain arrest: A distinct autosomal recessive developmental brain malformation phenotype. *American Journal of Medical Genetics Part A*, *167A*, 1089–1099.

Alarcon, A., Martinez-Biarge, M., Cabañas, F., Hernanz, A., Quero, J., & Garcia-Alix, A. (2013). Clinical, biochemical, and neuroimaging findings predict long-term neurodevelopmental outcome in symptomatic congenital cytomegalovirus infection. *Jornal de Pediatria*, *163*, 828–834.e1.

Alexander, I. E., Tauro, G. P., & Bankier, A. (1995). Fetal brain disruption sequence in sisters. *European Journal of Pediatrics*, *154*, 654–657.

Anbeek, P., Išgum, I., Van Kooij, B. J., Mol, C. P., Kersbergen, K. J., Groenendaal, F., . . . Benders, M. J. (2013). Automatic segmentation of eight tissue classes in neonatal brain MRI. *PLoS ONE*, *8*, e81895.

Averill, L. W., Kandula, V. V., Akyol, Y., & Epelman, M. (2015). Fetal brain magnetic resonance imaging findings In congenital cytomegalovirus infection with postnatal imaging correlation. *Seminars in Ultrasound, CT, and MR*, *36*, 476–486.

Bell, T. M., Field, E. J., & Narang, H. K. (1971). Zika virus infection of the central nervous system of mice. *Archiv für die gesamte Virusforschung*, *35*, 183–193.

Besnard, M., Eyrolle-Guignot, D., Guillemette-Artur, P., Lastère, S., Bost-Bezeaud, F., Marcelis, L., . . . Mallet, H.-P. (2016). Congenital cerebral malformations and dysfunction in fetuses and newborns following the 2013–2014 Zika virus epidemic in French Polynesia. *Euro Surveillance*, *21*, 13.

Bonnemann, C. G., & Meinecke, P. (2000). Dysmorphology fetal brain disruption. *Journal of Medical Genetics*, *27*, 273–274.

Brasil, P., Calvet, G. A., Siqueira, A. M., Wakimoto, M., de Sequeira, P. C., Nobre, A., . . . Jaenisch, T. (2016). Zika virus outbreak in rio de janeiro, Brazil: Clinical characterization, epidemiological and virological aspects. *PLOS Neglected Tropical Diseases*, *10*, 1–13.

Brasil, P., Pereira, J. P., Jr., Raja Gabaglia, C., Damasceno, L., Wakimoto, M., Ribeiro Nogueira, R. M., . . . Nielsen-Saines, K. (2016). Zika virus infection in pregnant women in rio de janeiro — preliminary report. *New England Journal of Medicine*, NEJMoa1602412.

Brasil, P., Pereira, J. P., Jr, Moreira, M. E., Ribeiro Nogueira, R. M., Damasceno, L., Wakimoto, M., . . . Nielsen-Saines, K. (2016). Zika virus infection in pregnant women in rio de janeiro. *New England Journal of Medicine*, *375*, 2321–2334.

Calvet, G., Aguiar, R. S., Melo, A. S., Sampaio, S. A., de Filippis, I., Fabri, A., . . . de Filippis, A. M. (2016). Detection and sequencing of Zika virus from amniotic fluid of fetuses with microcephaly in Brazil: A case study. *Lancet Infectious Diseases*, *16*, 653–660.

Campos, G. S., Bandeira, A. C., & Sardi, S. I. (2015). Zika virus outbreak, bahia. *Brazil Emerging Infectious Diseases*, *21*, 1885–1886.

Capretti, M. G., Lanari, M., Tani, G., Ancora, G., Sciutti, R., Marsico, C., . . . Faldella, G. (2014). Role of cerebral ultrasound and magnetic resonance imaging in newborns with congenital cytomegalovirus infection. *Brain and Development*, *36*, 203–211.

Carvalho, F. H., Cordeiro, K. M., Peixoto, A. B., Tonni, G., Moron, A. F., Feitosa, F. E., . . . Araujo Júnior, E. (2016). Associated ultrasonographic findings in fetuses with microcephaly due to suspected Zika virus (ZIKV) infection during pregnancy. *Prenatal Diagnosis*, *36*, 882–887.

Carvalho, M. D., Ferreira, L., Caldas, S., Linden, V. V. D., Coeli, R., & Ramos, F. (2016). Sensorineural hearing loss in a case of congenital Zika virus. *Brazilian Journal of Otorhinolaryngology*, pii: S1808-8694(16)30127-6. doi: 10.1016/j.bjorl.2016.06.001. [Epub ahead of print].

Carvalho, M. D., Miranda-Filho, D. B., van der Linden, V., Sobral, P. F., Ramos, R. C., Rocha, M., . . . Nunes, M. L. (2017). Sleep EEG patterns in infants with congenital Zika virus syndrome. *Clinical Neurophysiology*, *128*, 204–214.

Cavalheiro, S., Lopez, A., Serra, S., Da Cunha, A., da Costa, M. D., Moron, A., & Lederman, H. M. (2016). Microcephaly and Zika virus: Neonatal neuroradiological aspects. *Child's Nervous System*, *32*, 1057–1060.

Chang, C., Ortiz, K., Ansari, A., & Gershwin, M. E. (2016). The Zika outbreak of the 21st century. *Journal of Autoimmunity*, *68*, 1–13.

Cordeiro, M. T., Pena, L. J., Brito, C. A., Gil, L. H., & Marques, E. T. (2016). Positive IgM for Zika virus in the cerebrospinal fluid of 30 neonates with microcephaly in Brazil. *The Lancet*, *387*, 1811–1812.

Corona-Rivera, J. R., Corona-Rivera, E., Romero-Velarde, E., Hernández-Rocha, J., Bobadilla-Morales, L., & Corona-Rivera, A. (2001). Report and review of the fetal brain disruption sequence. *European Journal of Pediatrics*, *160*, 664–667.

Cugola, F. R., Fernandes, I. R., Russo, F. B., Freitas, B. C., Dias, J. L., Guimarães, K. P., . . . Beltrão-Braga, P. C. (2016). The Brazilian Zika virus strain causes birth defects in experimental models. *Nature*, *534*, 267–271.

Culjat, M., Darling, S. E., Nerurkar, V. R., Ching, N., Kumar, M., Min, S. K., . . . Melish, M. E. (2016). Clinical and imaging findings in an infant with zika embryopathy. *Clinical Infectious Diseases*, 1–7.

Dang, J., Tiwari, S. K., Lichinchi, G., Qin, Y., Patil, V. S., Eroshkin, A. M., & Rana, T. M. (2016). Zika virus depletes neural progenitors in human cerebral organoids through activation of the innate immune receptor TLR3. *Cell Stem Cell*, *19*, 258–265.

de Araújo, T. V., Rodrigues, L. C., de Alencar Ximenes, R. A., de Barros Miranda-Filho, D., Montarroyos, U. R., de Melo, A. P., . . . Martelli, C. M. (2016). Association between Zika virus infection and microcephaly in Brazil, January to May, 2016: Preliminary report of a case-control study. Lancet Infect. *Lancet Infectious Diseases*, *3099*, 1–8.

De Barros Miranda-Filho, D., Martelli, C. M., Ximenes, R. A., Araújo, T. V., Rocha, M. A., Ramos, R. C., . . . Rodrigues, L. C. (2016). Initial description of the presumed congenital Zika syndrome. *American Journal of Public Health*, *106*, 598–600.

de Fatima Vasco Aragao, M., van der Linden, V., Brainer-Lima, A. M., Coeli, R. R., Rocha, M. A., Sobral da Silva, P., . . . Valenca, M. M. (2016). Clinical features and neuroimaging (CT and MRI) findings in presumed Zika virus related congenital infection and microcephaly: Retrospective case series study. *BMJ*, *353*, i1901.

De Felice, C., Toti, P., Di Maggio, G., Parrini, S., & Bagnoli, F. (2001). Absence of the inferior labial and lingual frenula in Ehlers-Danlos syndrome. *The Lancet*, *357*, 1500–1502.

de Paula Freitas, B., de Oliveira Dias, J. R., Prazeres, J., Sacramento, G. A., Ko, A. I., Maia, M., & Belfort, R., Jr (2016). Ocular findings in infants with microcephaly associated with presumed zika virus congenital. *JAMA Ophthalmology*, *134*, 529–535.

Dick, G. W. A. (1952). Zika virus (I). Isolations and serological specificity. *Transactions of the Royal Society of Tropical Medicine and Hygiene*, *46*, 509–520.

Driggers, R. W., Ho, C.-Y., Korhonen, E. M., Kuivanen, S., Jääskeläinen, A. J., Smura, T., … Vapalahti, O. (2016). Zika virus infection with prolonged maternal viremia and fetal brain abnormalities. *New England Journal of Medicine*, *374*, 2142–2151.

Dudley, D. M., Aliota, M. T., Mohr, E. L., Weiler, A. M., Lehrer-Brey, G., Weisgrau, K. L., … O'Connor, D. H. (2016). A rhesus macaque model of Asian-lineage Zika virus infection. *Nature Communications*, *7*, 12204.

Fauci, A. S., & Morens, D. M. (2016). Zika virus in the americas — yet another arbovirus threat. *New England Journal of Medicine*, *374*, 601–604.

França, G. V., Schuler-Faccini, L., Oliveira, W. K., Henriques, C. M., Carmo, E. H., Pedi, V. D., & Victora, C. G. (2016). Congenital Zika virus syndrome in Brazil: A case series of the first 1501 Livebirths with complete investigation. *The Lancet*, *388*, 891–897.

Furdon, S. A., & Clark, D. A. (2003). Scalp hair characteristics in the newborn infant. *Advances in Neonatal Care*, *3*, 286–296.

Goodfellow, F. T., Tesla, B., Simchick, G., Zhao, Q., Hodge, T., Brindley, M. A., & Stice, S. L. (2016). Zika virus induced mortality and microcephaly in chicken embryos. *Stem Cells and Development*, *25*, 1691–1697.

Guillemette-Artur, P., Besnard, M., Eyrolle-Guignot, D., Jouannic, J. M., & Garel, C. (2016). Prenatal brain MRI of fetuses with Zika virus infection. *Pediatric Radiology*, *46*, 1032–1039.

Hanson, J., Smith, D., & Cohen, M. J. (1976). Prominent lateral palatine ridges: Developmental and clinical relevance. *Jornal de Pediatria*, *89*, 54–58.

Hazin, A. N., Poretti, A., Di Cavalcanti Souza Cruz, D., Tenorio, M., van der Linden, A., & Huisman, T. A. (2016). Computed tomographic findings in microcephaly associated with zika virus. *New England Journal of Medicine*, *374*, 2193–2195.

Honein, M. A., Dawson, A. L., Petersen, E. E., Jones, A. M., Lee, E. H., … Yazdy, M. M. (2017). Birth defects among fetuses and infants of US women with evidence of possible zika virus infection during pregnancy. *JAMA*, *317*, 59–68.

Huang, W.-C., Abraham, R., Shim, B.-S., Choe, H., & Page, D. T. (2016). Zika virus infection during the period of maximal brain growth causes microcephaly and corticospinal neuron apoptosis in wild-type mice. *Scientific Reports*, *6*, 34793.

Hughes, E. (1986). Congenital disruption: Microcephaly due to vascular In utero documentation. *Pediatrics*, *78*, 85.

Illingworth, R. (1965). Head circumference of infants related to body weight. *Archives of Disease in Childhood*, *40*, 672–676.

Jones, K. L. (1980). The Miller-Dieker syndrome. *Journal of Pediatrics*, *66*, 277–281.

Jones, K. L., Jones, M. C., Del Campo, M. (Eds.), (2013). *Smith's recognizable patterns of human malformation*. (7th ed.) Philadelphia, PA: Elsevier.

Kimura, S., & Kitagawa, T. (1986). Embryological development of human palmar, plantar, and digital flexion creases. *Anatomical Record*, *216*, 191–197.

Kumar, A., Kanojia, R. K., & Saili, A. (2014). Skin dimples. *International Journal of Dermatology*, *53*, 789–797.

Kurjak, A., Tikvica, A., Stanojevic, M., Miskovic, B., Ahmed, B., Azumendi, G., & Di Renzo, G. C. (2008). The assessment of fetal neurobehavior by three- dimensional and four-dimensional ultrasound. *journal of Maternal-Fetal and Neonatal Medicine*, *21*, 675–684.

Leal, C., Esteves-pereira, A. P., Nakamura-pereira, M., Torres, J. A., Themefilha, M., Maria, R., … Gama, S. G. (2016). Prevalence and risk factors related to preterm birth in Brazil. *Reproductive Health*, 13.

Li, H., Saucedo-Cuevas, L., Regla-Nava, J. A., Terskikh, A. V., Shresta, S., Gleeson, J. G., … Tang, W. (2016). Zika virus infects neural progenitors in the adult mouse brain and alters proliferation. *Stem Cell*, *19*, 1–6.

MacHet, L., Hüttenberger, B., Georgesco, G., Doré, C., Jamet, F., Bonnin-Goga, B., … Vaillant, L. (2010). Absence of inferior labial and lingual frenula in ehlers-danlos syndrome: A minor diagnostic criterion in french patients. *American Journal of Clinical Dermatology*, *11*, 269–273.

Martines, R. B., Bhatnagar, J., de Oliveira Ramos, A. M., Davi, H. P., Iglezias, S. D., Kanamura, C. T., … Zaki, S. R. (2016). Pathology of congenital Zika syndrome in Brazil: A case series. *The Lancet*, *388*, 898–904.

Melo, A. S., Aguiar, R. S., Amorim, M. M., Arruda, M. B., Melo, F. O., Ribeiro, S. T., … Tanuri, A. (2016). Congenital zika virus infection: Beyond neonatal microcephaly. *JAMA Neurology*, *73*, 1407–1416.

Microcephaly Epidemic Research Group (2016). Microcephaly epidemic research group. microcephaly in infants, pernambuco state, Brazil, 2015. *Emerging Infectious Diseases*, *22*, 1090–1093.

Miranda, H. A., 2nd, Costa, M. C., Frazão, M. A., Simão, N., Franchischini, S., & Moshfeghi, D. M. (2016). Expanded spectrum of congenital ocular findings in microcephaly with presumed zika infection. *Ophthalmology*, *123*, 1788–1794.

Mlakar, J., Korva, M., Tul, N., Popović, M., Poljšak-Prijatelj, M., Mraz, J., … Avšič, T. (2016). Zika virus associated with microcephaly. *New England Journal of Medicine*, *374*, 951–958.

Mochida, G. H., Ganesh, V. S., Felie, J. M., Gleason, D., Hill, R. S., Clapham, K. R., … Walsh, C. A. (2010). A homozygous mutation in the tight-junction protein JAM3 causes hemorrhagic destruction of the brain, subependymal calcification, and congenital cataracts. *American Journal of Human Genetics*, *87*, 882–889.

Moore, C., Weaver, D., & Bull, M. (1990). Fetal brain disruption sequence. *Jornal de Pediatria*, *116*, 383–386.

Moore, C. A., Staples, J. E., Dobyns, W. B., Pessoa, A., Ventura, C. V., Fonseca, E. B., … Rasmussen, S. A. (2016). Characterizing the pattern of anomalies in congenital zika syndrome for pediatric clinicians. *JAMA Pediatrics*, [Epub ahead of print].

Moura da Silva, A. A., Ganz, J. S., Sousa, P. D., Doriqui, M. J., Ribeiro, M. R., Branco, M. D., Queiroz, R. C., … Soares de Britto E Alves, M. T. (2016). Early growth and neurologic outcomes of infants with probable congenital zika virus syndrome. *Emerging Infectious Diseases*, *22*, 1953–1956.

Nishi, M., Miyake, H., Akashi, H., Shimizu, H., Tateyama, H., Chaki, R., & Nishi, M. …(1992). An index for proportion of head size to body mass during infancy. *Journal of Child Neurology*, *7*, 400–403.

Paciorkowski, A. R., Keppler-Noreuil, K., Robinson, L., Sullivan, C., Sajan, S., Christian, S. L., & Dobyns, W. B. (2013). Deletion 16p13.11 uncovers NDE1 mutations on the non-deleted homolog and extends the spectrum of severe microcephaly to include fetal brain disruption. *American Journal of Medical Genetics Part A*, *161*, 1523–1530.

PAHO. (2015). Neurological syndrome, congenital malformations, and Zika virus infection. Implications for public health in the Americas. *Pan American Health Organization*, 1–11.

Rasmussen, S. A., Jamieson, D. J., Honein, M. A., & Petersen, L. R. (2016). Zika virus and birth defects — reviewing the evidence for causality. *New England Journal of Medicine*, *384*, 1981–1987.

Rochelson, B., Vohra, N., Krantz, D., & Macri, V. J. (2006). Geometric morphometric analysis of shape outlines of the normal and abnormal fetal skull using three-dimensional sonographic multiplanar display. *Ultrasound in Obstetrics and Gynecology*, *27*, 167–172.

Russell, K., Oliver, S. E., Lewis, L., Barfield, W. D., Cragan, J., Meaney-Delman, D., … Rasmussen, S. A. (2016). Update: Interim guidance for the evaluation and management of infants with possible congenital zika virus infection—United States, August 2016. *MMWR Morbidity and Mortality Weekly Report*, *65*, 870–878.

Russell, L., Weaver, D., Bull, M., & Weinbaum, M. (1984). In utero brain destruction resulting in collapse of the fetal skull, microcephaly, scalp rugae, and neurologic impairment: The fetal brain disruption sequence. *American Journal of Medical Genetics*, *17*, 509–521.

Sadler, T. W. (2015). *Langman's medical embryology* (13th ed.). China: Wolters Kluwer Health.

Sarno, M., Sacramento, G. A., Khouri, R., do Rosário, M. S., Costa, F., Archanjo, G., … de Almeida, A. R. P. (2016). Zika virus infection and stillbirths: A case of hydrops fetalis, hydranencephaly and fetal demise. *PLOS Neglected Tropical Diseases*, *10*, 5–9.

Schram, A., Kroes, H. Y., Sollie, K., Timmer, B., Barth, P., & Essen, T. V. (2004). Clinical report hereditary fetal brain degeneration resembling fetal brain disruption sequence in two sibships. *American Journal of Medical Genetics Part A*, *182A*, 172–182.

Schuler-Faccini, L., Ribeiro, E. M., Feitosa, I. M., Horovitz, D. D., Cavalcanti, D. P., … Pessoa, A. (2016). Possible association between zika virus infection and microcephaly—Brazil, 2015. *MMWR Morbidity and Mortality Weekly Report*, *65*, 59–62.

Schuler-Faccini, L., Sanseverino, M., Vianna, F., da Silva, A. A., Larrandaburu, M., Marcolongo-Pereira, C., & Abeche, A. M. (2016). Zika virus: A new human teratogen? Implications for women reproductive age. *Clinical Pharmacology and Therapeutics*, *100*, 28–30.

Smith, D. W., & Gong, B. T. (1973). Scalp hair patterning as a clue to early fetal brain development. *Jornal de Pediatria*, *83*, 374–380.

Soares de Oliveira-Szejnfeld, P., Levine, D., Melo, A. S., Amorim, M. M., Batista, A. G., Chimelli, L., … Tovar-Moll, F. (2016). Congenital brain abnormalities and zika virus: What the radiologist can expect to see prenatally and postnatally. *Radiology*, *281*, 161584.

Soares de Souza, A., Moraes Dias, C., Braga, F. D., Terzian, A. C., Estofolete, C. F., Oliani, A. H., … Vaz-Oliani, D. C. (2016). Fetal infection by Zika virus in the third trimester—report of 2 cases. *Clinical Infectious Diseases*, *15*, 1622–1625.

Stevens, C. A., Carey, J. C., Shah, M., & Bagley, G. P. (1988). Development of human palmar and digital flexion creases. *Jornal de Pediatria*, *113*, 128–132.

Stratton, R. F., Dobyns, W. B., Airhart, S. D., & Ledbetter, D. H. (1984). New chromosomal syndrome: Miller-Dieker syndrome and monosomy 17p13. *Human Genetics*, *67*, 193–200.

Suy, A., Sulleiro, E., Rodó, C., Vázquez,, Bocanegra, C., Molina, I., … Carreras, E. (2016). Prolonged zika virus viremia during pregnancy. *The New England Journal of Medicine*, *375*, 2611–2613.

Tang, H., Hammack, C., Ogden, S. C., Wen, Z., Qian, X., Li, Y., … Ming, G. L. (2016). Zika virus infects human cortical neural progenitors and attenuates their growth. *Cell Stem Cell*, *18*, 587–590.

van der Eijk, A. A., van Genderen, P. J., Verdijk, R. M., Reusken, C. B., Mögling, R., van Kampen, J. J., … Koopmans, M. P. (2016). Miscarriage associated with zika virus infection. *New England Journal of Medicine*, *375*, 1002–1004.

van der Linden, V., Filho, E. L., Lins, O. G., van der Linden, A., Aragão Mde, F., Brainer-Lima, A. M., … Ramos, R. C. (2016). Congenital Zika syndrome with arthrogryposis: Retrospective case series study. *BMJ*, *354*, i3899.

Van der Linden, V., Pessoa, A., Dobyns, W., Barkovich, A. J., & Júnior, H. V. D. L. (2016). Description of 13 infants born during October 2015-January 2016 with congenital Zika virus infection without microcephaly at birth—Brazil. MMWR Morbidity and Mortality Weekly Report.

Ventura, C. V., Maia, M., Bravo-Filho, V., Góis, A. L., & Belfort, R. (2016). Zika virus in Brazil and macular atrophy in a child with microcephaly. *The Lancet*, *387*, 228.

Ventura, C. V., Maia, M., Travassos, S. B., Martins, T. T., Patriota, F., Nunes, M. E., … Belfort, R. (2016). Risk factors associated with the ophthalmoscopic findings identified in infants with presumed zika virus congenital infection. *JAMA Ophthalmology*, *134*, 912–918.

Ventura, C. V., Maia, M., Ventura, B. V., Van Der Linden, V., Araújo, E. B., Ramos, R. C., … Ventura, L. O. (2016). Ophthalmological findings in infants with microcephaly and presumable intra-uterus Zika virus infection. *Arquivos Brasileiros de Oftalmologia*, *79*, 1–3.

Verloes, A., Drunat, S., Gressens, P., & Passemard, S. (1993). Primary autosomal recessive microcephalies and Seckel syndrome spectrum disorders. In: R. A. Pagon, M. P. Adam, H. H. Ardinger, S. E. Wallace, A. Amemiya, L. J. H. Bean, T. D. Bird, N. Ledbetter, H. C. Mefford, R. J. H. Smith, & K. Stephens (Eds.). *GeneReviews® [Internet]* (pp. 1993–2017). Seattle, WA: University of Washington, Seattle.

Villar, J., Cheikh Ismail, L., Victora, C. G., Ohuma, E. O., Bertino, E., Altman, D. G., … Kennedy, S. H. (2014). International standards for newborn weight, length, and head circumference by gestational age and sex: The Newborn Cross-Sectional Study of the INTERGROWTH-21st Project. *The Lancet*, *384*, 857–868.

Villó, N., Beceiro, J., Cebrero, M., & de Frias, E. G. (2001). Fetal brain disruption sequence in a newborn infant with a history of cordocentesis at 21 weeks gestation. *Archives of Disease in Childhood Fetal and Neonatal Edition*, *84*, 63–64.

Zhang, F., Hammack, C., Ogden, S. C., Cheng, Y., Lee, E. M., Wen, Z., … Jin, P. (2016). Molecular signatures associated with ZIKV exposure in human cortical neural progenitors. *Nucleic Acids Research*, *44*, gkw765.

## SUPPORTING INFORMATION

Additional Supporting Information may be found online in the supporting information tab for this article.

**How to cite this article:** del Campo M, Feitosa IML, Ribeiro EM, et al. The phenotypic spectrum of congenital Zika syndrome. *Am J Med Genet Part A*. 2017;173A:841–857. https://doi.org/10.1002/ajmg.a.38170